Hindawi
Journal of Nanomaterials
Volume 2019, Article ID 8384794, 10 pages
https://doi.org/10.1155/2019/8384794

Research Article

Bandgap Engineering of Bilayer Ge/CdS Thin Films via Interlayer Diffusion under Different Annealing Temperatures

Faheem Amin,[1] **Syedah Afsheen Zahra**,[1] **Muhammad Sultan**,[2] **Sajjad Hussain Mirza**,[3] **and Fahad Azad**[1]

[1]*Department of Physics, School of Natural Sciences, National University of Sciences and Technology, Islamabad, Pakistan*
[2]*National Center for Physics, Islamabad, Pakistan*
[3]*LINAC Project, PINSTECH, Nilore Islamabad, Pakistan*

Correspondence should be addressed to Faheem Amin; faheem_phy@yahoo.com

Received 30 April 2018; Revised 6 November 2018; Accepted 23 December 2018; Published 24 March 2019

Guest Editor: Jiawei Gong

Bilayer thin films of Ge/CdS have been deposited on a glass substrate through thermal evaporation method. The obtained Ge/CdS samples were annealed at temperatures up to 400°C to observe the resulting effect on the structural changes in the film. The bandgap of the annealed films was found to increase with increasing annealing temperature which can be attributed to the increased interlayer diffusion. The interlayer diffusion was found to take effect above a temperature of 300°C which was confirmed by the Rutherford backscattering technique. Complementary XPS was done to investigate the surface stoichiometry of the bilayers.

1. Introduction

Multijunction solar cells are promising energy devices that are expected both to mitigate the imminent energy crisis and environmental menace [1–4]. However, for better understanding of the performance of these devices, a subtle knowledge of interfacial effects is required [5]. By carefully maneuvering the interface characteristics, the power conversion efficiency of the device can be enhanced. Moreover, the fact that theoretical efficiency is limited by the Schokley-Queisser limit exacerbated by the intrinsic losses makes the multijunction tandem solar cells with a tunable bandgap an ultimate choice [6, 7]. Multijunction solar cells on one hand can mitigate the thermal losses by utilizing several layers having different bandgap. On the other hand, the concatenation of absorber layers may enhance the efficiency of these solar cells significantly. For example, multijunction (III-V)/Ge semiconductor solar cells have been reported to manifest high efficiency of ~39% with up to four absorber layers [8]. The ability to engineer a bandgap of a multilayer thin-film solar cell is a technological milestone corroborated by the widespread research efforts over the past few decades. Many efforts have been put by the scientists to develop cascaded structures of intrinsic (Si and Ge) and extrinsic semiconductor compounds (metal chalcogenides [9–11] and perovskites [12, 13]). However, II-VI semiconductors have been rather less explored and needed further attention. In fact, heterojunctions of Ge/CdS have been developed through chemical vapor deposition of single crystal CdS epitaxial layers on (111) *p*-Ge substrates by Paorici et al. [14]. However, their aim was to study various methods to grow CdS on a Ge substrate rather than studying the impact of interface properties on the grown structures. Cadmium sulfide is a widely used material in various applications, such as photovoltaics, biomedical imaging, catalysis, IR detector, and space technologies, due to its wide bandgap of around 2.4 eV [15–17]. In solar cells, CdS has been vastly used as a buffer layer [18, 19]. Ge, on the other hand, is an indirect bandgap material (0.66 eV) and is commonly used as a bottom layer in multijunction solar cells.

In this work, we endeavor to study the behavior of Ge/CdS bilayer system to understand the underpinned mechanism for expected bandgap change. The bandgap of CdS has been reported to be sensitive to the oxygen concentration while

Ge content has been observed to increase the bandgap of alloyed $Cu_2ZnGe_xSn_{1-x}Q_4$ (Q = S,Se) [20, 21]. Therefore, we forecast a change in the bandgap of CdS upon alloying with Ge. The propitious alloying was achieved by the annealing of the bilayer films at various temperatures and diffusion of Ge into the CdS layer was observed. The interlayer diffusion is an important phenomenon as it results in the change in the thickness of layers and therefore the bandgap of materials. We specifically aimed at tailoring the thickness of the Ge layer as it has a relatively larger Bohr exciton radius (24.3 nm) [22] as compared to CdS (5.8 nm) [23].

2. Materials and Methods

All the reagents used in this study were of analytical grade. Powders of CdS (99.99%, M.Wt. 144.47 g.mol^{-1}) and Ge (99.999%, M.Wt. 72.64 g.mol^{-1}) were purchased from Sigma-Aldrich. The thin films were deposited on the soda lime glass substrate by thermally evaporating the precursors through resistive heating. The substrate was cleaned prior to deposition by sonicating at 70°C in dilute detergents for 10 minutes to avoid impurities that may cause defects in the films emanated due to contamination. The slides were then sonicated in deionized (DI) water for another 10 minutes to remove the detergent. Following this, the films were sonicated in pure ethanol for another 10 minutes. Finally, the slides were rinsed with DI water and blown dry with nitrogen.

For deposition, the vacuum level was maintained up to 1×10^{-5} mbar using diffusion pumps. The powders were melted in tungsten boats and evaporated to the slides. The substrates were held at room temperature and the substrate holder was rotated at 30 rpm for uniform deposition of the films. A 15 nm thick layer of Ge was deposited with an average deposition rate of 0.2 nm per second. After that, CdS was melted and evaporated to deposit a 20 nm thick layer on the Ge layer with an average deposition rate of 0.2 nm per second. The rate of deposition was monitored by the quartz crystal monitor placed inside the deposition chamber. The films were annealed in air at temperatures 100°C, 200°C, 300°C, 350°C, and 400°C inside a Muffle furnace for one hour before further use.

2.1. Structural Analysis

2.1.1. X-Ray Diffraction (XRD). X-ray diffraction (also called X-ray crystallography) was used to determine the structure of the prepared films. D8 Discover X-ray Diffractometer (Bruker AXS, Germany) was used with Cu-K_α radiation as a source of X-rays. The analysis was done at a grazing angle of 1°.

2.1.2. Scanning Electron Microscopy (SEM). The surface morphology of the thin films was studied by a Hitachi S-4800 FEG scanning electron microscope. The microscope is equipped with a Horiba EMAX EDS detector having an EMAX energy software for the elemental analysis of the materials.

2.1.3. Atomic Force Microscopy (AFM). The topological features of the films were analysed by the AFM microscopy technique using Quesant Universal SPM (Ambios Technology) that can image a lateral resolution down to 1.5 nm and a vertical resolution down to 0.05 nm. The images were taken in contact mode by using silicon nitride tips. The scans were taken over $5.0 \times 5.0\ \mu$m.

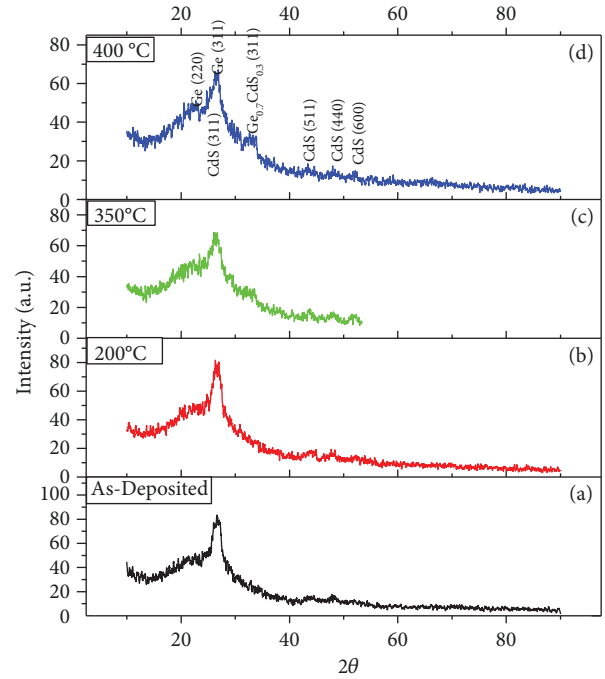

Figure 1: (a-d) Grazing incidence XRD pattern showing the peaks of various scatterings from the planes of Ge and CdS crystals. The spectra show the formation of FCC cubic structures of both Ge and CdS. The formation of a new mixed phase $Cd_{0.7}Ge_{0.3}S$ was also observed at high sintering temperature.

2.1.4. Rutherford Backscattering Spectroscopy (RBS). RBS depth profiling was done to determine the nonstoichiometric phases in the films. A beam of alpha particles of desired energy was generated by adjusting the voltage value of the beam accelerator, having a maximum capacity (5 MeV) of producing energetic He^{+2} particles, at an average energy of 2 MeV for alpha particle production. The samples were cut in pieces of size 1×1 cm^2 and taped on the sample holder. The chamber was evacuated prior to measurement. The geometry of target and detector was measured using CORNELL. The time required for recording a spectrum depends upon the charge collection. SIMNRA was used for the simulation of RBS spectra. The simulated spectrum is overlapped on the experimental spectrum to extract information about the thickness and composition of each layer. Ag-Cu alloy monolayer (with known backscattered energies) deposited on a glass substrate was used for the energy to channel scale conversion prior to sample measurement. The calculated values for keV(0) and keV/Ch were 56.820 keV and 1.1360, respectively. All of the subsequent simulations for the different samples were done using these values. After the successful channel to energy scale calibration, the expected target information was provided to the software and the simulation was run. The simulated spectrum thus generated was overlapped

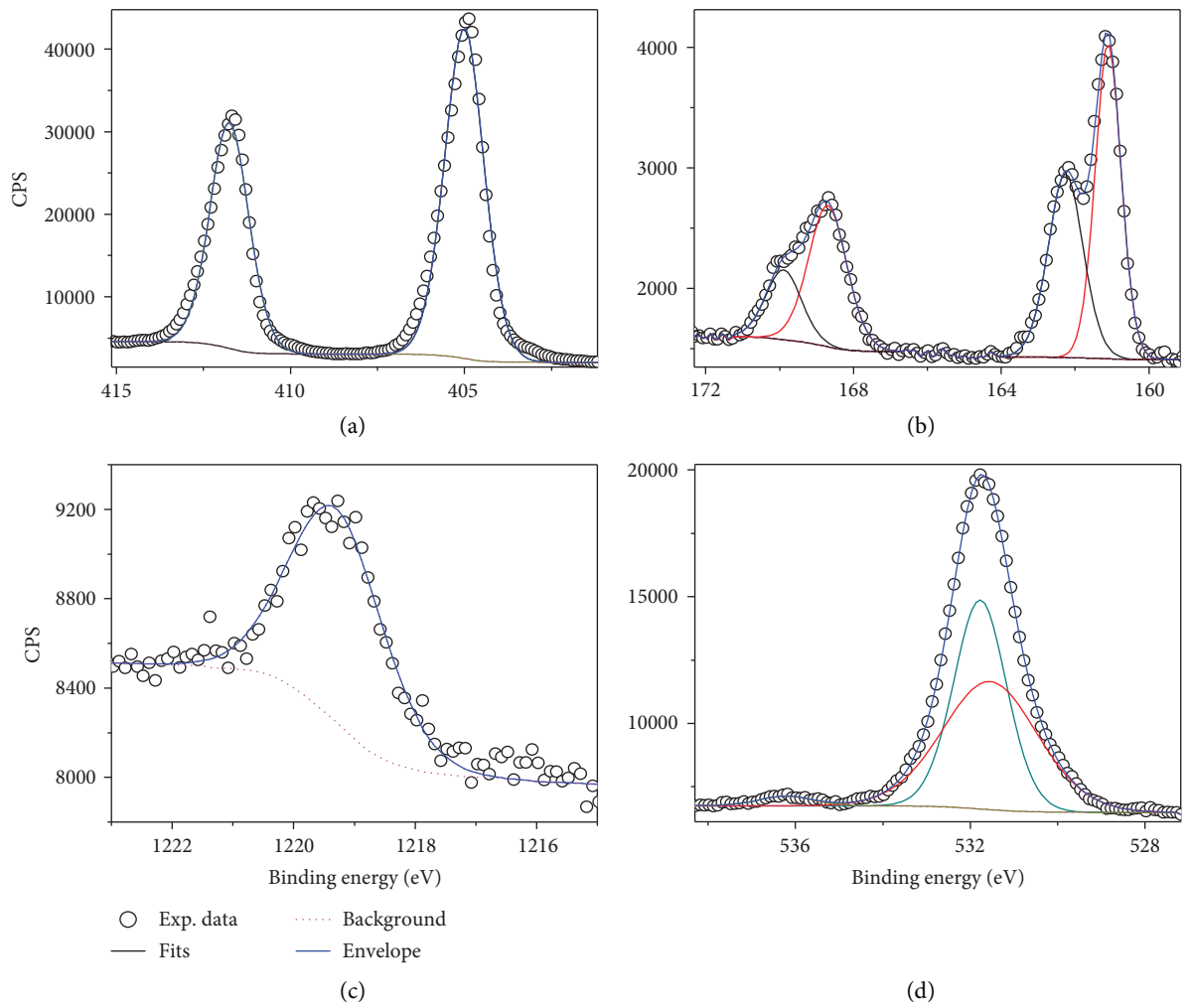

FIGURE 2: High resolution (a) Cd3d core level spectrum, (b) S2p XPS spectra of CdS film, and (c) Ge2p spectrum of underneath Ge spectrum. The surface oxides are shown in (d).

on the experimental spectrum and the thicknesses of layers were calculated.

2.2. Spectroscopic Analysis

2.2.1. UV-Visible Spectroscopy. The optical properties of the films were studied through the Labomed UV-visible spectrophotometer. The films were held perpendicular to the beam for the analysis. The obtained data was converted to transmittance and further analysed for the calculation of the band-gap via the Tauc plot.

2.2.2. Photoluminescence. A photoluminescence analysis was performed to determine the emission characteristics of the prepared thin films. The Kimmon 30 mW He-Cd laser (325 nm) was used as an excitation source. A photomultiplier (PMT), a focal length monochromator (500 mm), and the lock-in amplifier were used for the acquisition of the spectrum.

2.2.3. XPS Spectroscopy. The XPS spectroscopy was performed using a standard omicron system equipped with a monochromatic Al Ka 1486.7 eV X-ray source and the Argus hemispherical electron spectrometer with 128 channel MCP detector. The CasaXPS software was used for data analysis and curve fitting. C1s was used for the calibration of binding energies of all spectra.

3. Results and Discussion

Figures 1(a)–1(d) show the XRD patterns of the annealed films at various temperatures. X-rays were made incident at a grazing angle of 1° on the film to minimize the contribution from the underlying amorphous glass substrate. The broader hump at around 26° can be attributed to the superposition of the glass substrate and (311) contribution from Ge and CdS. A small spike at about 32.8° (not labeled) correspond to (400) in samples annealed at 350°C and 400°C. Moreover, the intensity of (311) the peak was found to lower for these samples. This can be probably due to the formation of a new mixed phase, CdGeS. A tiny spike before the main peak at about 21° corresponds to (200) plane in Ge. Further peaks at 43.2°, 48.1°, and 52.8° correspond to (511), (400), and

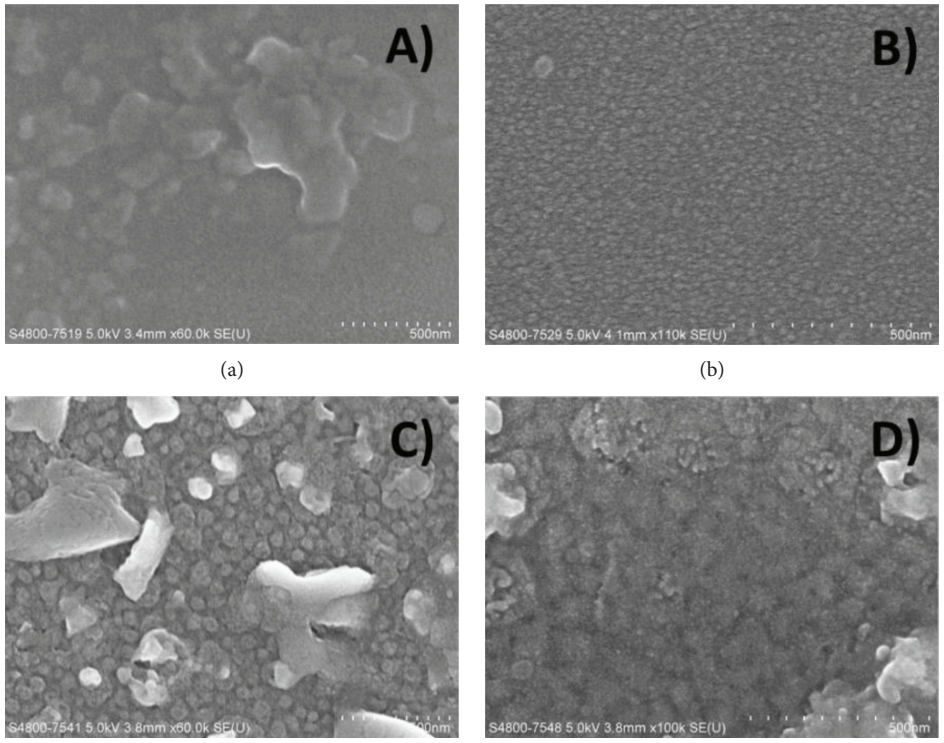

Figure 3: SEM images of sintered samples:(a) the as-deposited film, (b) film annealed at 200°C, (c) film annealed at 350°C, and (d) film annealed at 400°C. Different phases of materials are also developing with sintering temperature. The scale corresponding to (a) is 1 μm while to (b) and (c) is 300 nm.

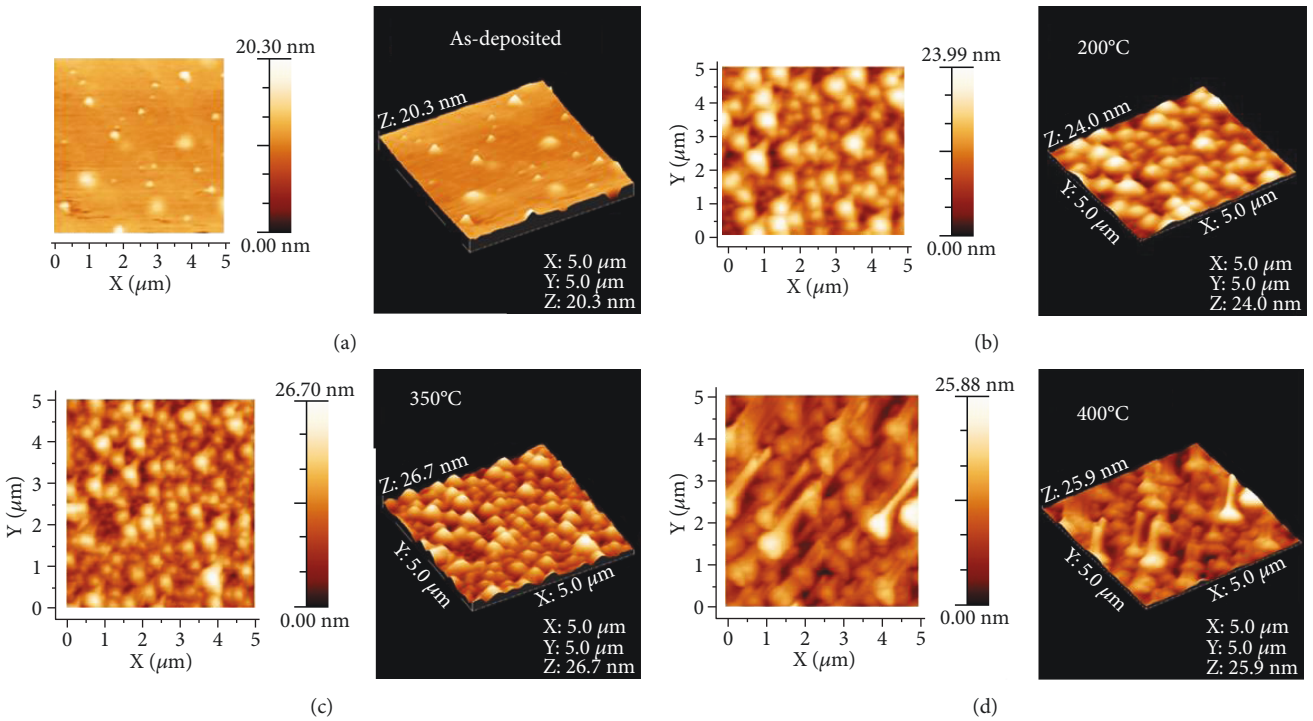

Figure 4: (a-d) AFM images of the annealed films. The samples annealed at the different temperatures show the increased roughness with the annealing temperature. The sample annealed at 400°C shows the associated oxides which can be confirmed by XPS.

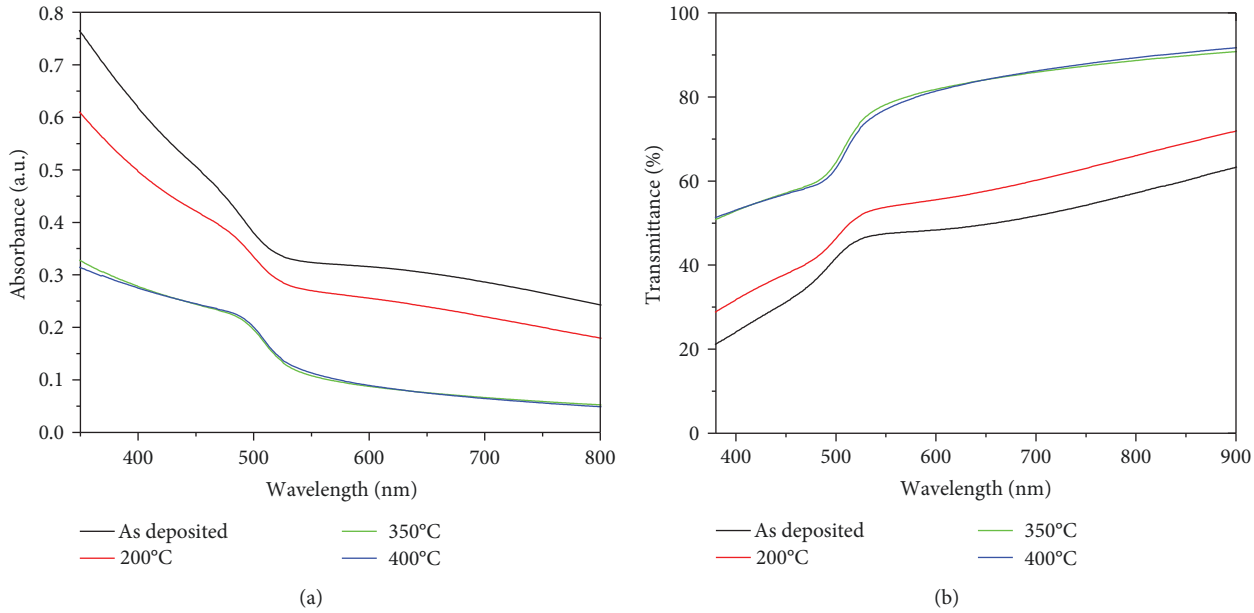

Figure 5: Absorbance (a) and transmittance (b) of the films annealed at the different temperatures.

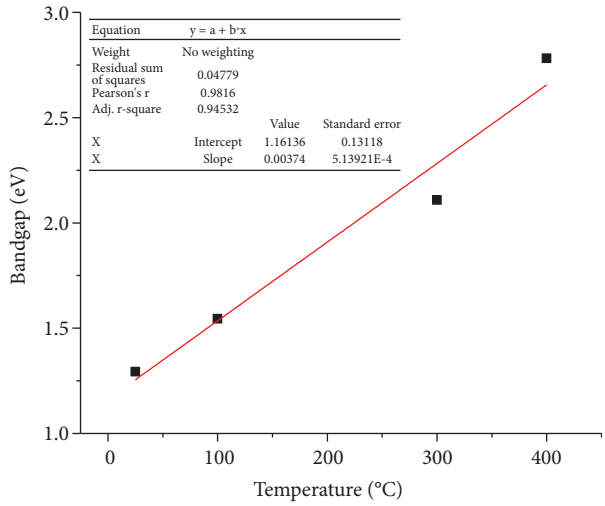

Figure 6: Optical bandgap as a function of sintering temperature. The Tauc plot was used for the determination of bandgap.

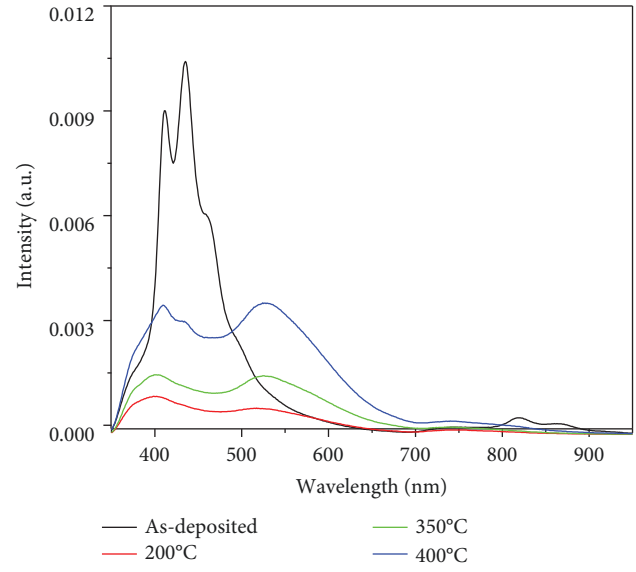

Figure 7: Photoluminescence spectra of annealed thin films.

(600) planes in CdS, respectively. From the XRD spectrum, it can be elucidated that FCC structured germanium with a space group of Fm-3m (225) and FCC structured CdS with a space group of F-43m (216) were developed on the films.

XPS analysis of the sample annealed at 400°C was done to get further insight of diffusion. Figure 2 shows the high resolution Cd3d, S2p, Ge2p, and O1s spectra of a CdS/Ge bilayer sample. All the high resolution spectra were fitted by the Voigt line shape using the Shirley background. The Cd3d line shape can be fitted by a single symmetric peak corresponding to CdS bonding. On the other hand, the S2p spectra can be fitted by two components consisting of the CdS bond along with one additional contribution at about 168.5 eV possibly from the oxidation of sulfur to the sulphate group. Ge2p peak was also observable by XPS which indicates that the CdS layer is very thin so that one can see the underneath Ge layer. As seen in Figure 2(d), the O1s also shows two peaks, one mainly from the surface-adsorbed oxygen species and one additional contribution possibly from the oxidized surface of the substrate, i.e., SiO_2. The Ge signal was found at a depth of around 10 nm which indicates the diffusion of Ge into the CdS layer.

Figure 3 shows the SEM images of the (a) as-prepared film, (b) film annealed at 200°C, and (c) film annealed at 350°C. Annealing is found favourable for the grain growth and grain boundaries and increase more rapidly above 300°C.

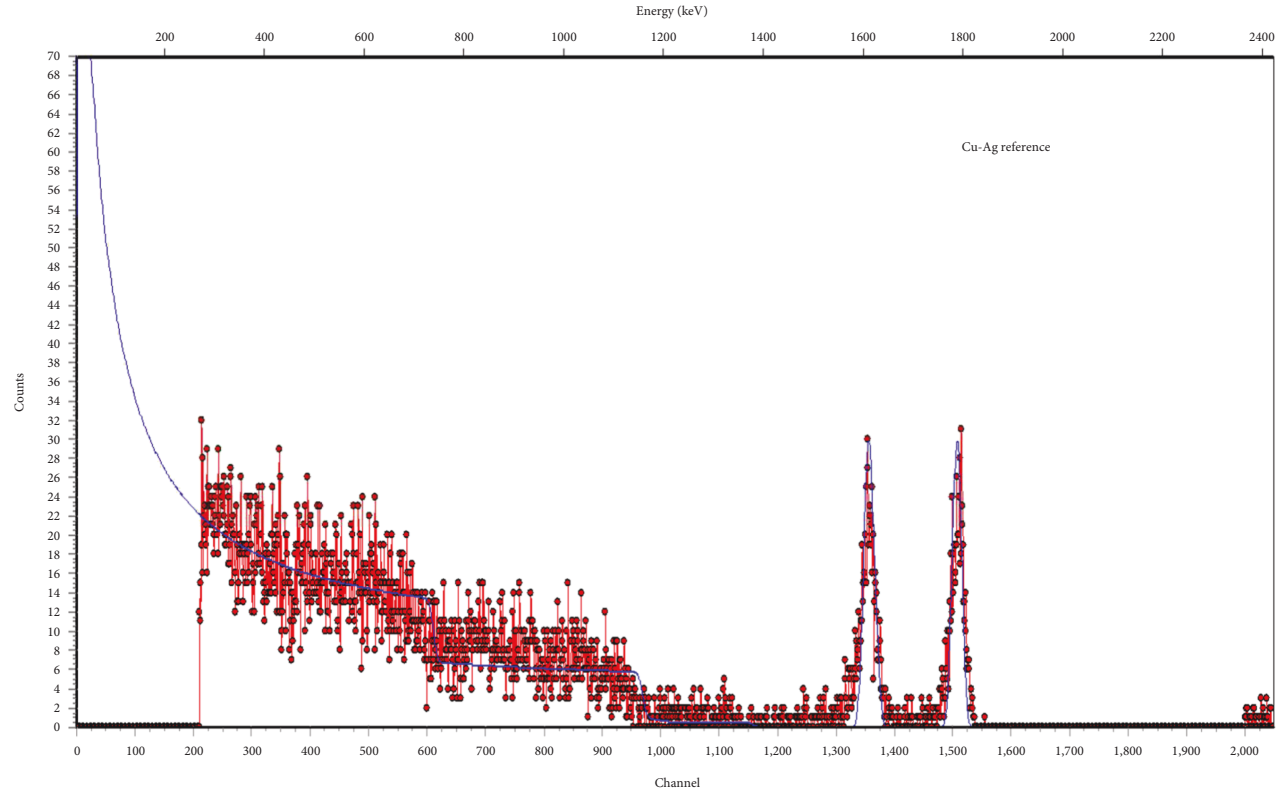

(a)

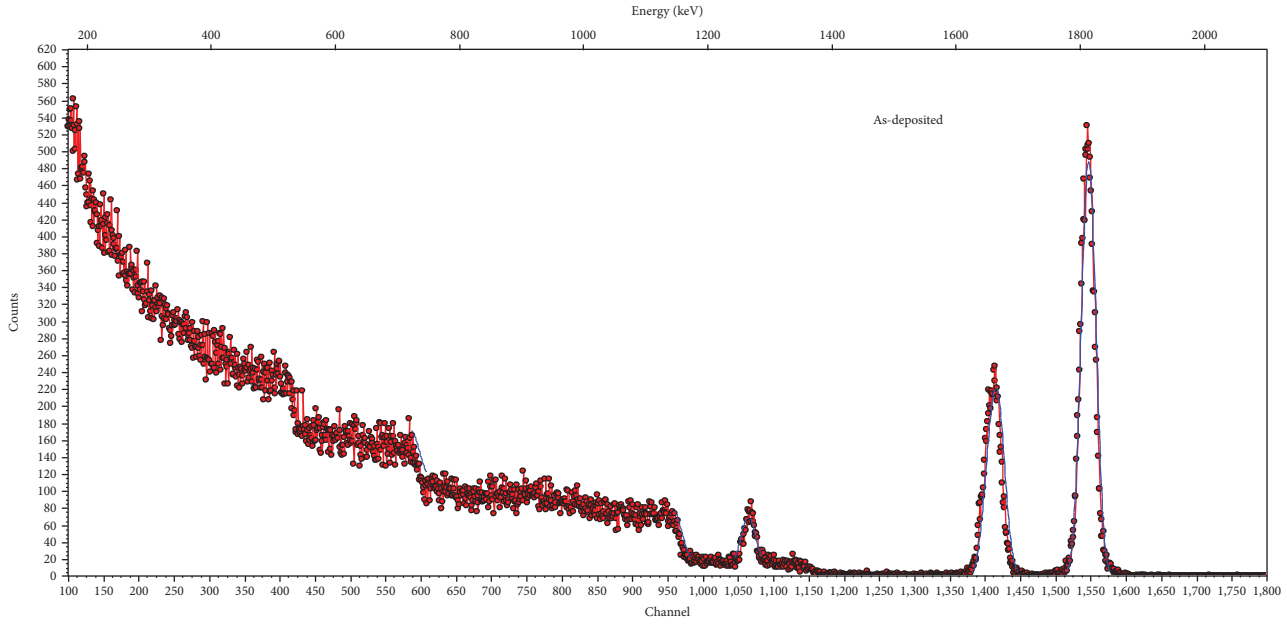

(b)

Figure 8: Continued.

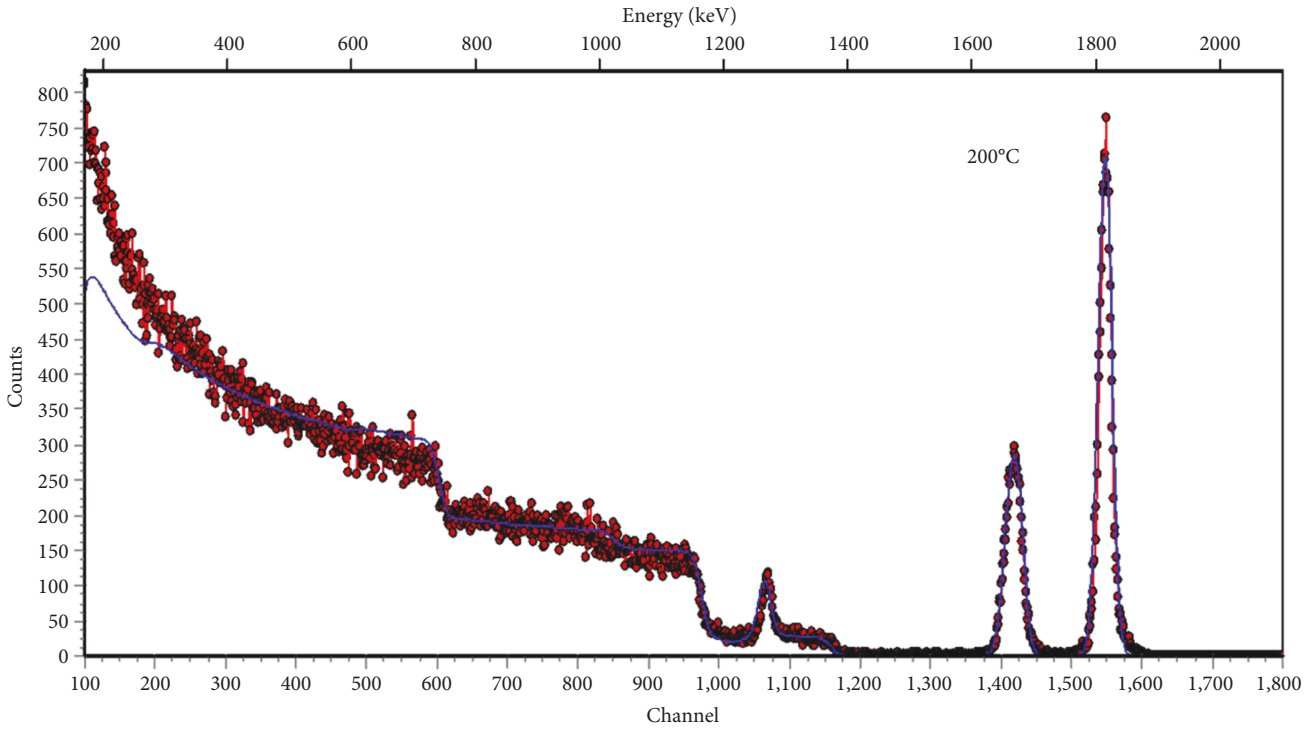

(c)

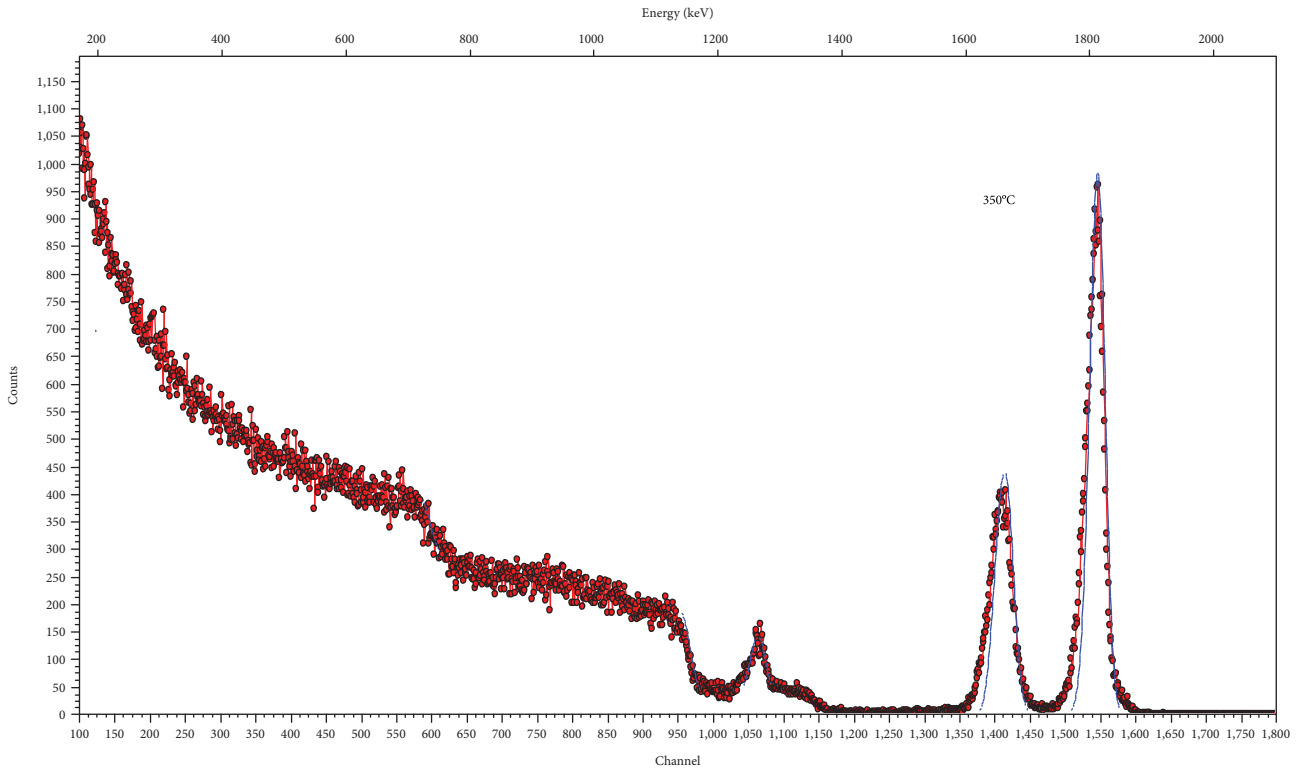

(d)

Figure 8: Continued.

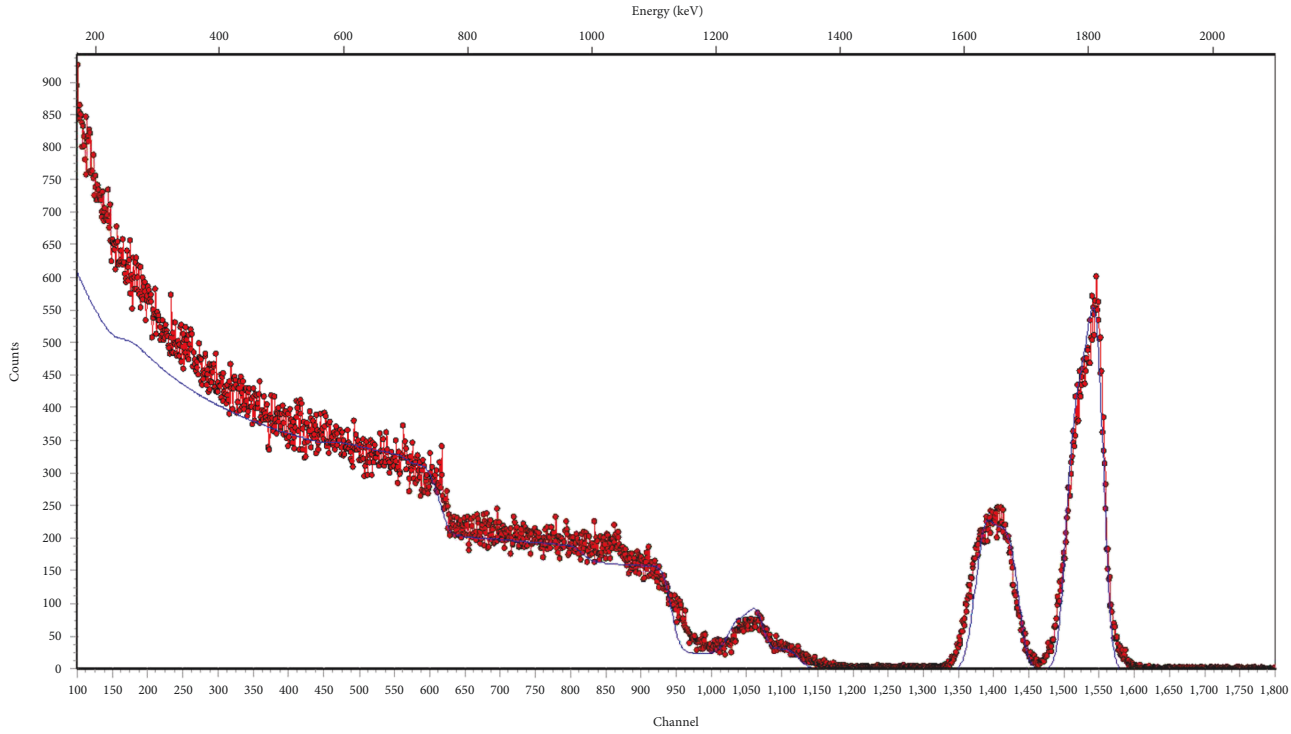

(e)

Figure 8: (a-e) Simulated curves of all the samples for RBS analysis. The Copper-Silver reference was used.

Figures 4(a)–4(d) show the surface morphology of bilayer Ge and CdS system. The surface roughness was found to increase more rapidly, i.e., from 20.3 nm to 24.0 nm, for annealing until 200°C. A further increase of the annealing temperature to 400°C was found to influence the surface roughness by 26.7 nm little as compared to 200°C. This can be attributed to the oxidation of the surface at 400°C. The observed changes in the surface roughness can be possibly due to an increase in the crystallite size and improved film uniformity [24].

Figure 5(a) shows the absorption spectra of the annealed samples while Figure 5(b) shows the transmission spectra. The UV/Vis spectroscopy showed two peaks of as-prepared sample, a weak shoulder at around 500 nm and a broader hump peaked at about 640 nm. The weak shoulder was found to become stronger and blueshifted with the increasing annealing temperature while the broader hump was found to disappear for the annealed films. The optical bandgap of the as-prepared and annealed samples was calculated by the Tauc plot and plotted in Figure 6. The bandgap was found to increase with the annealing temperature.

Figure 7 shows the photoluminescence of the thin films at different temperatures. The peak at 396 nm in all the samples corresponds to the electron-hole recombination near the bandgap edge. The peak near 450 nm in the as-prepared sample corresponds to sulfur vacancy, while peak near 530 nm in the heat-treated samples may be assigned to surface trap-induced emission. It can be seen with the increase in temperature that the green emission shift to the red from 450 nm to 525 nm is the result of interlayer diffusion and removal of shallow traps [25].

Figure 8 shows the RBS fittings for as-deposited and annealed samples. The distinct peaks for all of the three possible elements can be marked separately at different energies. The CdS and Ge peaks are marked and well fitted for as-deposited samples confirming the successful deposition of CdS and Ge. Sulfur (S) shows a relatively less intense peak around 1250 KeV which can be attributed to the smaller atomic mass of sulfur. One can see that the prominent effect of annealing appears at 400°C as the broadening of individual peaks with a decrease in their height which confirms the diffusion of both layers as a result of annealing. The composition of mixed phase was found out to be $Cd_{0.7}Ge_{0.3}S$ which can also be observed in the XRD pattern of the samples annealed at 400°C.

4. Conclusions

Bilayer thin films of Ge/CdS have been successfully fabricated. The structure of the conformed films was verified through XRD analysis. The analysis was done at a grazing angle to minimize the contribution from underlying substrate. The major peak at (400°C) can be attributed to the superposition of CdS and Ge films. The XPS analysis confirmed the formation of oxides at temperatures above 350°C. From the SEM analysis, it was found that the grain boundaries of the annealed films keep on growing with the annealing temperature. The surface roughness was found to increase with the annealing temperature attributed to the

formation of bigger grains. The Rutherford Backscattering (RBS) analysis showed that the annealing of the thin films resulted in the interlayer diffusion across the CdS and Ge layers emanating the bandgap narrowing in the case of Ge layer. The presence of different phases was confirmed both by XRD and RBS analysis. The optical bandgap was calculated using the Tauc plot and was found to increase with the annealing temperature. The photoluminescence data showed that the green luminescence increases with the increase in temperature due to the removal of shallow traps. The photoelectron spectroscopy revealed the presence of both surface-adsorbed and oxidized surface which leads to the bandgap widening as expected. However, the phenomenon of diffusion and the development of phases need to be further investigated.

Data Availability

No data were used to support this study.

Conflicts of Interest

No conflict of interest exists and the submitting author is responsible for coauthors declaring their interests.

Acknowledgments

The authors Faheem Amin and Syedah Afsheen Zahra, are thankful to the Higher Education Commission, Pakistan, for providing a Start-up Grant (PD-IPFP/HRD/-HEC/2013/1994) for this research work. Authors Faheem Amin, Syedah Afsheen Zahra, and Muhammad Sultan, are also thankful to the National Center for Physics, Islamabad, for granting access to the research facilities.

References

[1] M. Yamaguchi and S. Wakamatsu, "Super-high efficiency solar cell R&D program in Japan," in *Proceedings of the 25th IEEE Photovoltaic Specialists Conference*, p. 167, New York, 1996.

[2] J. Zeitouny, E. A. Katz, A. Dollet, and A. Vossier, "Band gap engineering of multi-junction solar cells: Effects of Series Resistances and Solar Concentration," *Scientific Reports*, vol. 7, no. 1, article 1766, 2017.

[3] M. Hosenuzzaman, N. A. Rahim, J. Selvaraj, M. Hasanuzzaman, A. B. M. A. Malek, and A. Nahar, "Global prospects, progress, policies, and environmental impact of solar photovoltaic power generation," *Renewable and Sustainable Energy Reviews*, vol. 41, pp. 284–297, 2015.

[4] M. M. Aman, K. H. Solangi, M. S. Hossain et al., "A review of safety, health and environmental (SHE) issues of solar energy system," *Renewable and Sustainable Energy Reviews*, vol. 41, pp. 1190–1204, 2015.

[5] A. W. Czanderna, "Stability of interfaces in solar energy materials," *Solar Energy Materials*, vol. 5, no. 4, pp. 349–377, 1981.

[6] W. Shockley and H. J. Queisser, "Detailed balance limit of efficiency of *p*-n junction solar cells," *Journal of Applied Physics*, vol. 32, no. 3, pp. 510–519, 1961.

[7] L. C. Hirst and N. J. Ekins-Daukes, "Fundamental losses in solar cells," *Progress in Photovoltaics: Research and Applications*, vol. 19, no. 3, pp. 286–293, 2011.

[8] T. B. Leijtens, K. A. Pasanna, R. McGehee, and D. E, "Opportunities and challenges for tandem solar cells using metal halide perovskite semiconductors," *Nature Energy*, vol. 3, no. 10, pp. 828–838, 2018.

[9] R. S. Bauer and J. C. Mikkelsen Jr., "Surface processes controlling MBE heterojunction formation: GaAs (100)/Ge interfaces," *Journal of Vacuum Science and Technology*, vol. 21, no. 2, pp. 491–497, 1982.

[10] A. D. Katnani, N. G. Stoffel, R. R. Daniels, T.-X. Zhao, and G. Margaritondo, "Heterojunction interface formation: Si on Ge, GaAs, and CdS," *Journal of Vacuum Science and Technology A*, vol. 1, no. 2, pp. 692–694, 1983.

[11] D. W. Niles, M. Tang, J. McKinley, R. Zanoni, and G. Margaritondo, "Schottky-like correction terms in heterojunction band lineups," *Physical Review B*, vol. 38, no. 15, pp. 10949–10952, 1988.

[12] W. Zi, X. Ren, X. Ren, Q. Wei, F. Gao, and S. Liu, "Perovskite/-germanium tandem: a potential high efficiency thin film solar cell design," *Optics Communications*, vol. 380, pp. 1–5, 2016.

[13] S. Hu, M. McDaniel, D. Posadas et al., "Monolithic integration of perovskites on Ge(001) by atomic layer deposition: a case study with $SrHf_xTi_{1-x}O_3$," *MRS Communications*, vol. 6, no. 3, pp. 125–132, 2016.

[14] C. Paorici, C. Pelosi, G. Bolzoni, and G. Zuccalli, "Epitaxial growth of cadmium sulphide on (111) germanium substrates," *Journal of Materials Science*, vol. 10, no. 12, pp. 2117–2123, 1975.

[15] Q. Wu, J. Hou, H. Zhao et al., "Charge recombination control for high efficiency CdS/CdSe quantum dot co-sensitized solar cells with multi-ZnS layers," *Dalton Transactions*, vol. 47, no. 7, pp. 2214–2221, 2018.

[16] D. Kathirvela, N. Suriyanarayanan, S. Prabahar, and S. Srikanth, "Structural, Electrical and Optical Properties of CdS Thin Films by Vacuum Evaporation Deposition," *Journal of Ovonic Research*, vol. 7, no. 4, pp. 83–92, 2011.

[17] T. Torimoto, S. Nagakubo, M. Nishizawa, and H. Yoneyama, "Photoelectrochemical properties of size-quantized CdS thin films prepared by an electrochemical method," *Langmuir*, vol. 14, no. 25, pp. 7077–7081, 1998.

[18] N. Romeo, A. Bosio, R. Tedeschi, A. Romeo, and V. Canevari, "A highly efficient and stable CdTe/CdS thin film solar cell," *Solar Energy Materials and Solar Cells*, vol. 58, no. 2, pp. 209–218, 1999.

[19] N. Memarian, S. M. Rozati, I. Concina, and A. Vomiero, "Deposition of Nanostructured CdS Thin Films by Thermal Evaporation Method: Effect of Substrate Temperature," *Materials*, vol. 10, no. 7, p. 773, 2017.

[20] M. A. Islam, M. S. Hossain, M. M. Aliyu et al., "Growth of Wide Bandgap CdS Thin Films as Window Layers of Ultra-Thin CdTe Solar Cells," in *The 22nd International Photovoltaic Science and Engineering Conference*, Hangzhou, China, November 2012.

[21] D. B. Khadka and J. Kim, "Band gap engineering of alloyed $Cu_2ZnGe_xSn_{1-x}Q_4$ (Q = S,se) films for solar cell," *Journal of Physical Chemistry C*, vol. 119, no. 4, pp. 1706–1713, 2015.

[22] G. Gu, M. Burghard, G. T. Kim et al., "Growth and electrical transport of Ge nanowires," *Journal of Applied Physics*, vol. 90, no. 11, pp. 5747–5751, 2001.

[23] L. V. Titova, T. B. Hoang, H. E. Jackson et al., "Low-temperature photoluminescence imaging and time-resolved spectroscopy of single CdS nanowires," *Applied Physics Letters*, vol. 89, no. 5, article 053119, 2006.

[24] W.-D. Park, "Structural and optical properties of thermally annealed Nanocrystalline CdS thin films," *Journal of the Korean Physical Society*, vol. 54, no. 5, pp. 1793–1797, 2009.

[25] L. Saravanan, S. Diwakar, R. Mohankumar, A. Pandurangan, and R. Jayavel, "Synthesis, Structural and Optical Properties of PVP Encapsulated CdS Nanoparticles," *Nanomaterials and Nanotechnology*, vol. 1, no. 2, pp. 17–48, 2011.